Nanocomposites based on halloysite nanotubes and sulphated galactan from red seaweed *Gloiopeltis*: Properties and delivery capacity of sodium diclofenac

Giuseppe Cavallaro [*], Giuseppe Lazzara, Stefana Milioto

[a] *Dipartimento di Fisica e Chimica, Università degli Studi di Palermo, Viale delle Scienze, pad. 17, 90128 Palermo, Italy*
[b] *Consorzio Interuniversitario Nazionale per la Scienza e Tecnologia dei Materiali, INSTM, Via G. Giusti, 9, I-50121 Firenze, Italy*

ABSTRACT

We developed novel composite films based on biocompatible components, such as halloysite clay nanotubes and sulphated galactan (Funori) from red seaweed *Gloiopeltis*. The filling of the nanotubes within the sulphated galactan matrix was carried out by a green protocol (aqueous casting method) assuring that Funori/halloysite nanocomposites can be totally considered as sustainable materials. The amount of halloysite in the composites was systematically changed to explore the effects of the nanofiller concentration on the mesoscopic properties of the films. We observed that the halloysite content significantly affects the initial water contact angle and the light attenuation coefficient of the Funori based films. These results were interpreted according to SEM images, which showed that the surface morphologies of the nanocomposites depend on the halloysite amounts filled within the polymeric matrix. The mechanical characterization of the nanocomposites was conducted by tensile experiments performed using a linear stress ramp. Moreover, tensile tests were conducted in oscillatory regime at variable temperature to investigate the viscoelastic properties of the nanocomposites.

Finally, we filled the biopolymeric matrix with halloysite nanotubes containing sodium diclofenac. The drug release kinetics from the nanocomposites at variable halloysite contents were studied to evaluate their suitability as oral dissolving films for pharmaceutical applications.

1. Introduction

In recent years, the filling of biopolymeric matrix with nanoparticles has been extensively explored to fabricate composite biomaterials useful for several technological and biomedical applications [1–6]. Among the nanoparticles, nanoclays have been largely employed as fillers of biopolymers because of their versatile physico-chemical characteristics, which include tunable surface charge, different morphologies, and large specific area [7]. Moreover, nanoclays can be obtained from natural geological deposits and, consequently, they are significantly cheaper with respect to the synthetic nanoparticles. Remarkably, clay nanoparticles can be considered as ecocompatible and low toxic materials ensuring their use for drug delivery, tissue engineering and wound healing [8,9]. Halloysite (HNT) represents a suitable nanoclay for several biomedical applications because of its hollow tubular shape. Due to their geometrical characteristics, halloysite was used as catalytic support [10–13] and emulsifying agent of Pickering emulsions [14–17].

Interestingly, the HNT cavity can be filled with biologically active molecules driving to the production of modified nanotubes with targeted functionalities useful within pharmaceutics and biomedicine [18–22]. Within this, it should be noted that halloysite clay nanotubes are appropriate for biomedical purposes because of their weak toxicity demonstrated by both in vivo and in vivo biological experiments [23,24]. Halloysite was successful employed as additive for scaffolds in tissue engineering [25–27] as well as nanocarrier of drug molecules [28–33]. It was demonstrated that HNT can be used as drug delivery system with controlled release properties on dependence of external stimuli [34,35]. Literature reports that HNT loaded with active molecules can be filled within a polymeric matrix driving to obtain bionanocomposite films useful within materials science [36–39] and medical field [34,40,41]. In this regard, antimicrobial and antioxidant films were obtained by combining pectin with halloysite nanotubes containing salicylic acid [36] and peppermint essential oil [37]. Nanocomposite films based on chitosan and HNT loaded with norfloxacin

* Corresponding author at: Dipartimento di Fisica e Chimica, Università degli Studi di Palermo, Viale delle Scienze, pad. 17, 90128 Palermo, Italy.
E-mail address: giuseppe.cavallaro@unipa.it (G. Cavallaro).

exhibited a sustained release capacity of the drug with a consequent enhancement of the therapeutic benefits [40]. Layered hybrid tablets were obtained by blending alginate and chitosan filled with HNT containing sodium diclofenac [34]. The filling with halloysite nanotubes can improve the properties of the polymers in terms of mechanical resistance and thermal stability. These effects are strongly related to the specific polymer/HNT interactions as well as to the nanofiller content, which affect the morphological characteristics of the corresponding nanocomposites [36,42]. Mater-Bi filled with 10 wt% of halloysite exhibited improvements of the tensile properties with respect to the pristine biopolymer because of the uniform distribution of the nanotubes within the matrix [40]. Opposite effects were detected for the Mater-Bi/HNT films with a larger filler concentration (30 wt%) due to the formation of clusters between the clay nanotubes [42].

Here, we investigated the filling of Funori matrix with halloysite with the aim to produce composite films suitable for pharmaceutical applications. Funori is a natural polymer extracted from the red seaweed *Gloiopeltis*. Chemically, Funori is a sulphated galactan where the main chain is composed by two repeating units of (1,3)-β-Dgalactopyranose and (1,4)-α-(L or D)-galactopyranose. Literature reports that Funori was extensively employed for restoration and conservation of artworks [43], while its use for the development of biopolymeric films is unexplored. Concerning the applications within Cultural Heriate, Funori based glue was used as water-soluble adhesive of historical wooden samples [44]. Remarkably, the addition of clay nanotubes within the Funori glue can improve the adhesion performances [44].

In this paper, the combination of Funori and halloysite was explored to fabricate sustainable films with variable physico-chemical properties and sustained delivery capacity for biologically active molecules.

2. Experimental

2.1. Materials and methods

Halloysite nanotubes (HNT) were provided by Sigma Aldrich. Funori was obtained from CTS srl (Italy).

The tensile properties of the bionanocomposites were studied by Dynamic Mechanical Analysis (DMA) using the DMA Q800 apparatus (TA Instruments). The tests were conducted under a controlled stress ramp (1 MPa min^{-1}) at 25.0 ± 0.1 °C. Furthermore, DMA experiments were carried out in the oscillatory regime by heating the sample from 25 to 150 °C under a scanning rate of 3 °C min^{-1}. The frequency of the oscillation was set at 1.0 Hz, while the amplitude stress was fixed at 2 MPa.

UV–Vis spectroscopy experiments were carried out using a Analytic Jena SpecordS 600 BU UV–vis spectrophotometer.

The wettability characteristics of the composite films were analyzed through the contact angle apparatus (OCA 20, Data Physics Instruments) equipped with a video measuring system having a high-resolution CCD camera. The contact angle (ϑ) of water in air was measured by the sessile drop method at 25.0 ± 0.1 °C.

Thermogravimetric analysis (TGA) was carried out by means of the Q5000 IR (TA Instruments) instrument. The thermogravimetric experiments were performed under inert atmosphere using Nitrogen flows of 25 and 10 cm^3 min^{-1} for the sample and the balance, respectively. The samples were heated from 25 to 700 °C with a scanning rate of 20 °C min^{-1}.

SEM analyses were performed by using a SEM microscope (Desktop SEM Phenom PRO X PHENOM) with beam energy ranging between 4.8 and 20.5 kV. The films were preliminarily coated with gold to avoid charging effects.

2.2. Preparation of Funori/HNTs bionanocomposites

The Funori/HNTs composite films were prepared through the aqueous casting procedure, which revealed successful in the fabrication of nanocomposites based on several ionic and non-ionic biopolymers (pectin, alginate, starch, cellulose ethers) and halloysite clay nanotubes [36,42,45].

Firstly, 30 g of Funori were dispersed in 500 g of water by magnetically stirring for 2 h at 80 °C. The obtained dispersion, which appeared yellowish and viscous, was filtered through a cellulosic filter (porosity of 0.45 μm) under vacuum to remove residual impurities. Then, the Funori dispersion was ultrasonicated for 5 min and magnetically stirred for 30 min. We estimated that the Funori content in the dispersion is equal to 5.5 ± 0.1 wt%. This value was determined by the gravimetric method comparing the masses of the Funori dispersion before and after the complete water evaporation, which was carried out at 120 °C.

Afterwards, variable amounts of halloysite nanotubes were added to 20 g of the Funori dispersion in order to systematically change the biopolymer/HNT mass ratio. The Funori/HNT aqueous mixtures were kept under magnetically stirring overnight at 25 °C. Finally, the mixtures were ultrasonicated for 5 min to avoid clustering effects.

Finally, the Funori/HNT aqueous suspensions were poured in glass Petri dishes (diameter of 9 cm), which were kept in an oven at 50 °C until the water evaporation was complete. The nanocomposite films were easily removed from the glass support and stored in a desiccator at 25 °C and relative humidity of 75 %. The halloysite mass concentration (C_{HNT}) in the bionanocomposites was varied up to 30 wt%. Fig. 1 shows the optical photos of the films based on pure Funori and Funori/HNT (C_{HNT} = 30 wt%). We observed that the addition of halloysite in the Funori matrix does not generate significant variations on macroscopic characteristics of the biopolymeric film.

Moreover, functional nanocomposite films with filler contents of 10 and 25 wt% were prepared by filling the Funori matrix with HNT previously loaded with sodium diclofenac, which can act as antimicrobial and anti-inflammatory drug [46] The HNT loading with sodium diclofenac was conducted by the vacuum assisted procedure reported elsewhere [34].

3. Results and discussion

3.1. Wettability and surface morphology of Funori/Halloysite nanocomposites

The influence of the halloysite addition on the wettability properties of Funori based films were investigated by water contact angle measurements. Fig. 2a displays the images of the water droplets immediately after their deposition on pristine Funori and Funori/HNT nanocomposite (C_{HNT} = 5 and 15 wt%) films.

As a general result, we observed that the filling of Funori matrix with halloysite induces a reduction of the initial water contact angle highlighting an enhancement of the wettability of the film surface. This effect is consistent with the presence of HNT at the interface being that clay nanotubes are hydrophilic. Similar results were detected for nanocomposites based on halloysite and several biopolymers, such as pectin [36], chitosan [45] and alginate [45].

As shown in Fig. 2b, the initial contact angle vs C_{HNT} data present a reduction trend for halloysite concentration up to 15 wt% in agreement with the enrichment of the clay nanotubes on the surface of the Funori based film. Further increases of the nanofiller content (C_{HNT} = 25 and 30 wt%) did not generate significant variations of the initial contact angle, which is constantly equal to ca. 56°. This finding might be related to the formation of halloysite clusters causing an enhancement of the film roughness, which contribute to the surface hydrophobization. Within this, literature reports that the aggregation of hydrophilic nanoparticles at the interface of polymeric films can generate hydrophobization effects on the surface due to variations of the roughness [47]. On this basis, we can hypothesize that the wettability of Funori/HNT nanocomposites is not altered for C_{HNT} ranging between 15 and 30 wt% because the mentioned processes (HNT enrichment on the surface and HNT clustering) simultaneously occur and their corresponding
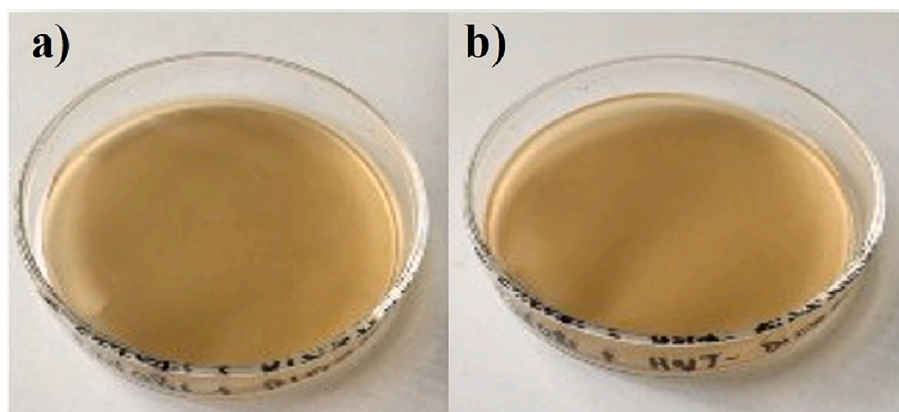
Fig. 1. Optical photos of films based on pristine Funori (a) and Funori/HNT nanocomposite at $C_{HNT} = 30$ wt% (b).
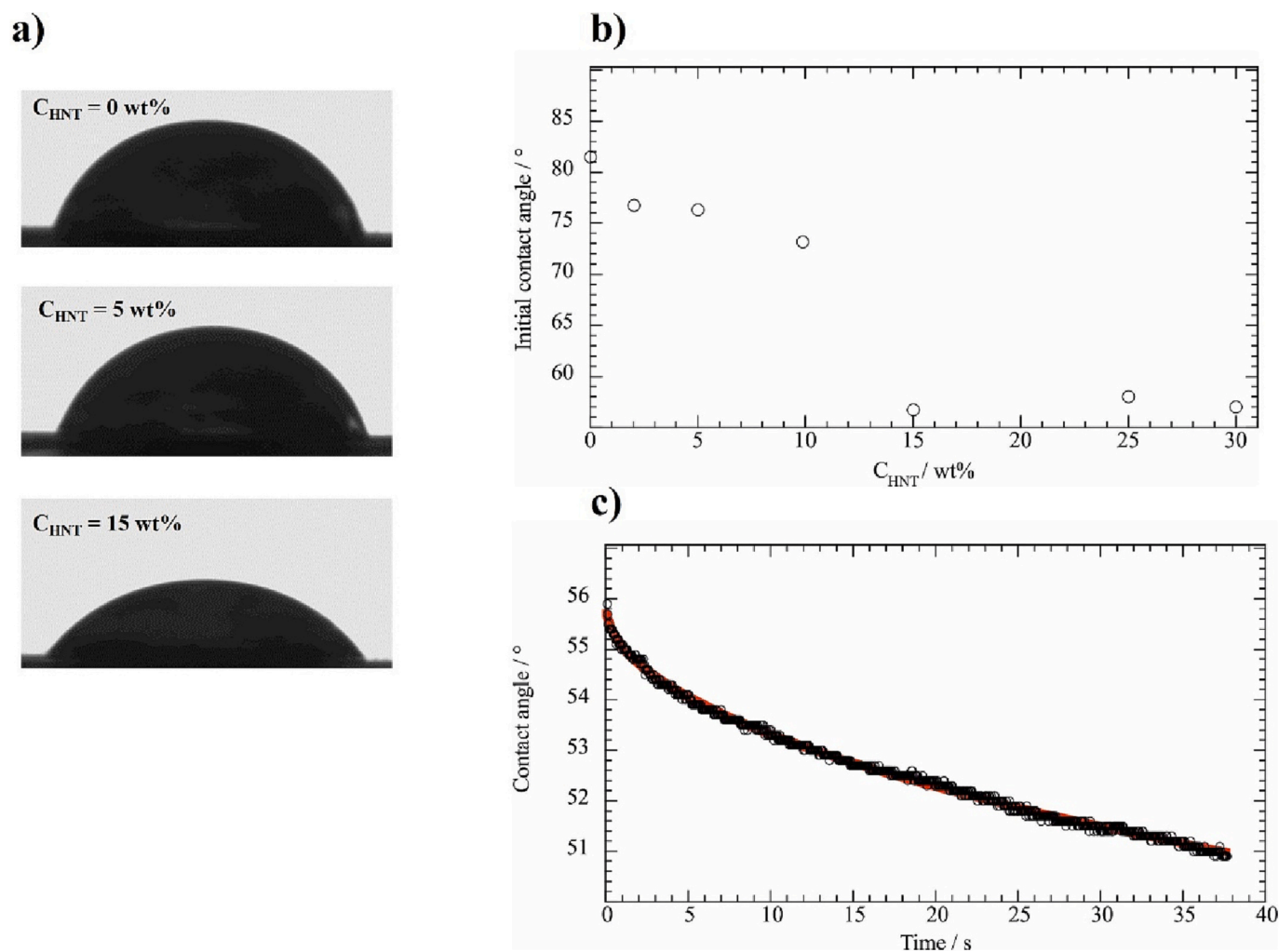

Fig. 2. a) Images of water droplet immediately after their deposition on Funori/HNT nanocomposites with variable composition; b) Initial water contact angle as a function of the HNT content; c) Dependence of the water contact angle on time for Funori/HNT nanocomposite ($C_{HNT} = 15$ wt%). Red line represents the fitting according to Eq. (1). (For interpretation of the references to colour in this figure legend, the reader is referred to the web version of this article.)

effects are counterbalanced.

The interpretation of the wettability results was supported by SEM images (Fig. 3), which allowed us to investigate the surface morphologies of Funori/HNT nanocomposites.

As shown in Fig. 3a, halloysite nanotubes are well dispersed within the Funori matrix for the composite film with $C_{HNT} = 5$ wt%. This

nanocomposite does not show any aggregation process between the nanotubes, which are randomly distributed into the polymeric matrix. Oppositely, the SEM image of Funori/HNT composite with a larger HNT concentration ($C_{HNT} = 25$ wt%) evidenced the presence of clusters between the clay nanotubes on the film surface.

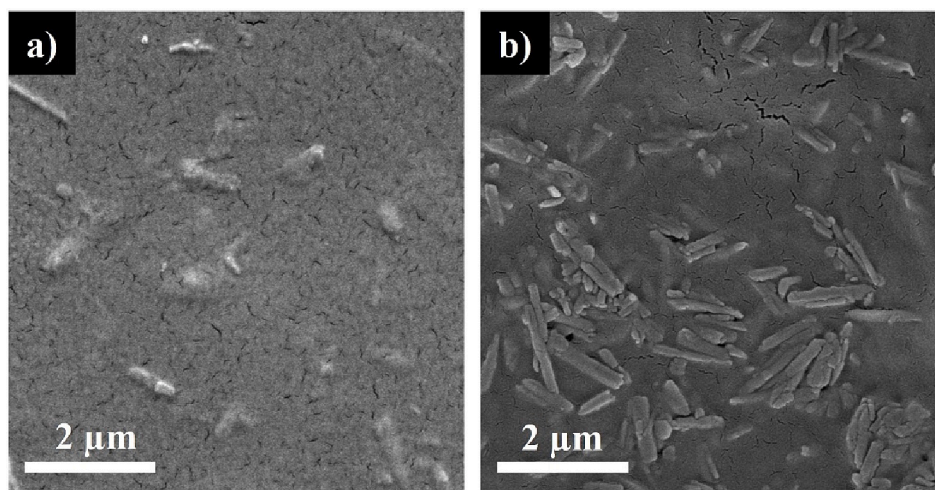We studied the kinetic evolution of the water contact angle to

Fig. 3. SEM images of Funori/HNT nanocomposites with halloysite contents of 5 wt% (a) and 25 wt% (b).

explore the absorption and spreading mechanisms on the surface of Funori/HNT composite films. As example, Fig. 2c shows the dependence of the contact angle on time for the nanocomposite with $C_{HNT} = 15$ wt%. The contact angle (θ) vs time (t) curves were successfully analyzed by using a semiquantitative approach [48], which can be expressed as.

$$\theta = \theta_i \bullet exp. \left(-k_\theta \bullet t^{n(\theta)} \right) \qquad (1)$$

where θ_i is the initial contact angle, while k_θ and $n(\theta)$ are the kinetic constant and the exponential parameter, respectively. It should be noted that the value of the exponential parameter reflects the contributions of absorption and spreading processes. Specifically, $n(\theta)$ can range between 0 (pure absorption) and 1 (pure spreading).

Table 1 reports the fitting parameters obtained by the analysis of the time evolution trends of water contact angle. We detected that $n(\theta)$ values range between 0 and 1 highlighting that both absorption and spreading processes occur for all the materials. As concerns pristine Funori, we estimated $n(\theta) = 0.407$, while the $n(\theta)$ values range between ca. 0.38 and 0.58 for Funori/HNT nanocomposite. These results indicate that the absorption and spreading mechanisms contribute almost equally for all the Funori based films.

3.2. Effects of halloysite addition on the transparency of Funori films

We investigated the effects of halloysite nanotubes on the transparency of Funori based films by spetroscopy experiments performed within the Vis region (400–800 nm). Fig. 4a shows the attenuation coefficient (k) as a function of the wavelenght for Funori/HNT nanocomposites with variable nanofiller concentration. It should be noted that k values were calculated by the absorbance (A) data using the following equation.

$$k = A/(2.3 \cdot D) \qquad (2)$$
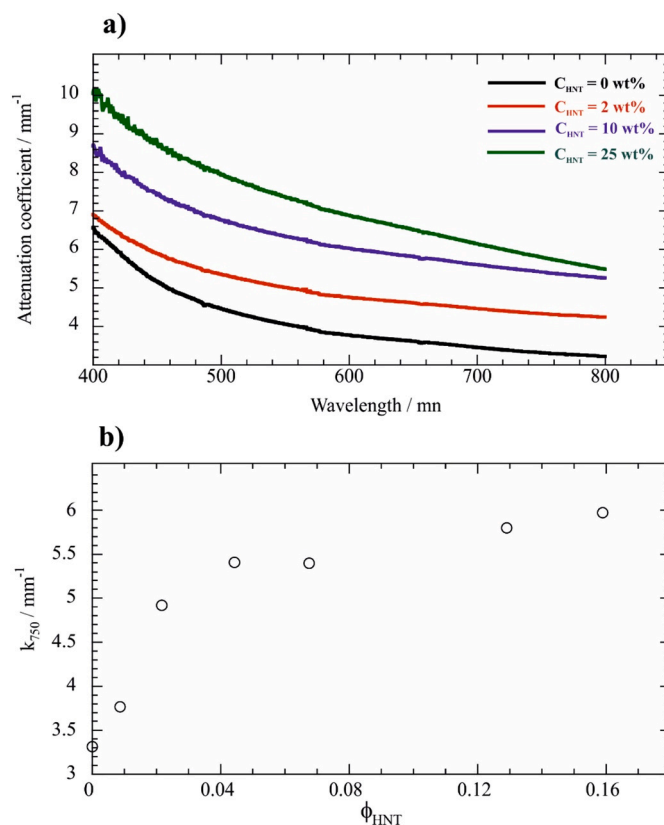
where D is the thickness of the film.

Fig. 4. a) Attenuation coefficient as a function of the wavelength for Funori/HNT films with variable filler content. b) Dependence of the attenuation coefficient at 750 nm on the HNT volume fraction for Funori/HNT nanocomposites.

As a general result, the addition of halloysite enhanced the attenuation coefficient of Funori highlighting that the nanocomposites exhibited a lower transparency with respect to that of the film based on the pristine biopolymer. This effect is stronger by increasing the halloysite concentration of the hybrid materials. Similar results were detected for pectin/HNT and hydroxylpropylcellulose/HNT nanocomposites [49,50]. Interestingly, the transparency represents a mesoscopic property that can provide information on the structural characteristics of the nanocomposite materials. [48] To this purpose, we considered the attenuation coefficient values at 750 nm (k_{750}) where the

Table 1
Fitting parameters obtained from the analysis of the contact angle vs time trends.

HNT content/wt%	k_θ / s^n	$n(\theta)$
0	$(3.21 \pm 0.06) \bullet 10^{-2}$	0.407 ± 0.003
2	$(0.84 \pm 0.02) \bullet 10^{-2}$	0.579 ± 0.004
5	$(0.88 \pm 0.02) \bullet 10^{-2}$	0.559 ± 0.005
10	$(1.73 \pm 0.03) \bullet 10^{-2}$	0.387 ± 0.005
15	$(1.46 \pm 0.02) \bullet 10^{-2}$	0.505 ± 0.003
25	$(2.33 \pm 0.05) \bullet 10^{-2}$	0.478 ± 0.004
30	$(2.57 \pm 0.05) \bullet 10^{-2}$	0.377 ± 0.005

transmittance data reflect only light scattering processes. Fig. 4b shows the dependence of k_{750} on the halloysite volume fraction (ϕ_{HNT}). We observed that k_{750} linearly increases with the halloysite concentration for $\phi_{HNT} \leq 0.5$ indicating that the nanotubes are uniformly distributed within the polymeric matrix. [48] The further increase of halloysite generated a deviation from the linearity in agreement with the formation of clusters between halloysite nanotubes. This finding is consistent with the contact angle data (Fig. 2b) as well as with the surface morphologies of the nanocomposites (Fig. 3).

3.3. Mechanical properties of Funori/Halloysite nanocomposites

The mechanical properties of Funori/HNT composite films were studied through DMA experiments in tension mode. Specifically, tensile tests were conducted by using a linear stress ramp. As examples, Fig. 5 shows the stress vs strain curves for films based on pristine Funori and Funori/HNT nanocomposite with 10 wt% of nanofiller.

The analysis of the stress vs strain curves allowed us to determine the tensile performances of the films in terms of elastic modulus, stress at breaking point and ultimate elongation. Fig. 5 shows that the nanocomposite possesses a better elastic modulus compared with that of pristine Funori as demonstrated by the higher slope of the linear trend in the elastic region. On the other hand, the addition of HNT reduced the stress and the elongation at the break point of Funori based film. As evidenced in Fig. 6, the tensile properties of the Funori/HNT composite films are strongly dependent on the nanofiller content.

We detected that the elastic modulus is improved by increasing the HNT concentration. The nanocomposite with $C_{HNT} = 25$ wt% exhibited an elastic modulus ca. 4 times larger compared with that of pure Funori. Nevertheless, it is important to note that the Funori filling with small amounts of HNT ($C_{HNT} = 2$ wt%) generated a relevant enhancement (ca. 40 %) of the elastic modulus. Regarding the stress at breaking point and the ultimate elongation, we observed that both properties evidenced a reduction by increasing the HNT concentration of the nanocomposite films. Compared to pure Funori, the stress at break and the ultimate elongation were reduced by ca. 41 % and 84 %, respectively, for the Funori/HNT nanocomposite with the largest filler concentration ($C_{HNT} = 25$ wt%). It should be noted that the decrease of the ultimate elongation can be attributed to the Funori/HNT interactions, which prevent the sliding between the polymeric chains [51]. Contrary to the elastic modulus and the ultimate elongation, the addition of small amounts of HNT ($C_{HNT} = 2$ wt%) in the polymeric matrix generated a negligible variation (ca. 3 %) on the stress at break.

In addition, tensile experiments were performed in the oscillatory regime to determine the viscoelastic properties of the films. Table 2 reports the storage (G') and loss (G'') moduli at 25 °C of Funori and Funori/HNT nanocomposites. Based on the rheological moduli, we calculated $\tan(\delta)$ as G''/G'. We observed that $\tan(\delta)$ is slightly reduced by the HNT addition within the polymeric matrix indicating that the elastic component is marginally more relevant in the nanocomposites with respect to pristine Funori.

The effects of the temperature variations on the viscoelastic characteristics of the films were studied within the range 25–150 °C. As shown in Fig. 7, the $\tan(\delta)$ vs temperature trends for both pristine Funori and Funori/HNT nanocomposite ($C_{HNT} = 10$ wt%) evidenced a peak in the region between ca. 60 and 80 °C that could be attributed to structural changes of the polymer, which becomes more amorphous. This process might reflect the glass transition of Funori. Interestingly, the peak intensity was decreased by the HNT addition highlighting that the nanocomposite possesses a higher capacity to store energy during the structural transition of the polymer. Similar results were detected for the glass transition of the polymer in the chitosan/HNT nanocomposites [45,52]. Moreover, we observed that the increase of the nanofiller content shifts the Funori glass transition towards lower temperatures. As shown in Table 2, the temperature at $\tan(\delta)$ peak was reduced by ca. 15 °C in the nanocomposite with the largest HNT content ($C_{HNT} = 25$ wt %) compared to that of pristine polymer.

3.4. Release of sodium diclofenac from Funori/halloysite composite

The loading of halloysite cavity with active molecules represents an easy strategy to obtain functional nanofillers for polymeric materials [49]. In this work, halloysite was loaded with sodium diclofenac in order to achieve nanotubes with antimicrobial and anti-inflammatory actions useful for pharmaceutical and biomedical applications. The amount of drug encapsulated within the halloysite lumen was determined by thermogravimetric (TG) experiments. Fig. 8 compares the TG curves of HNT loaded with sodium diclofenac and the corresponding pristine components (HNT and sodium diclofenac).

The drug encapsulation within the lumen reduced the residual mass at 700 °C (MR_{700}) of halloysite. In detail, we calculated MR_{700} values of 82.3 and 79.9 wt% before and after the loading, respectively. As reported elsewhere [30], we estimated the encapsulated drug (7.01 ± 0.15 wt%) through the rule of mixtures by considering MR_{700} values and moisture contents (mass losses from 25 to 150 °C) of pristine components and HNT loaded with sodium diclofenac.
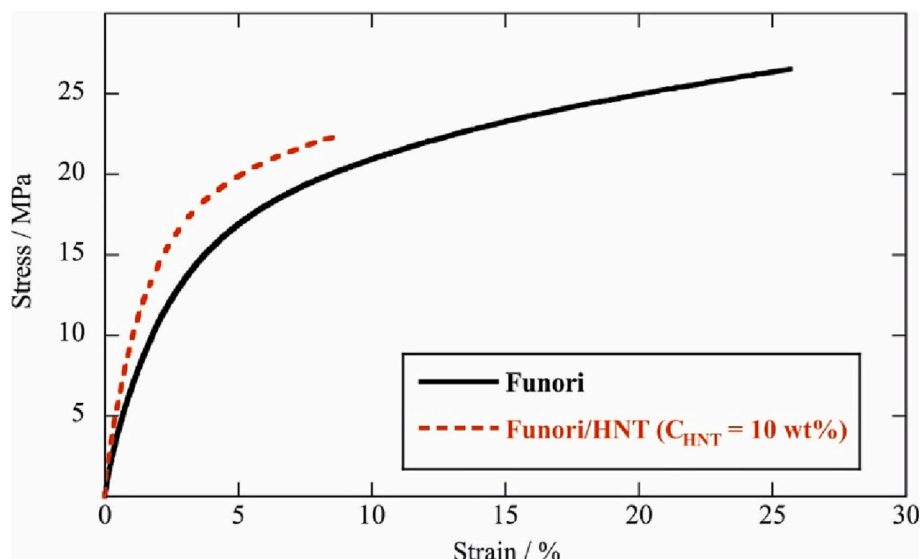

Fig. 5. Stress vs strain curves of films based on pristine Funori and Funori/HNT with halloysite content of 10 wt%.
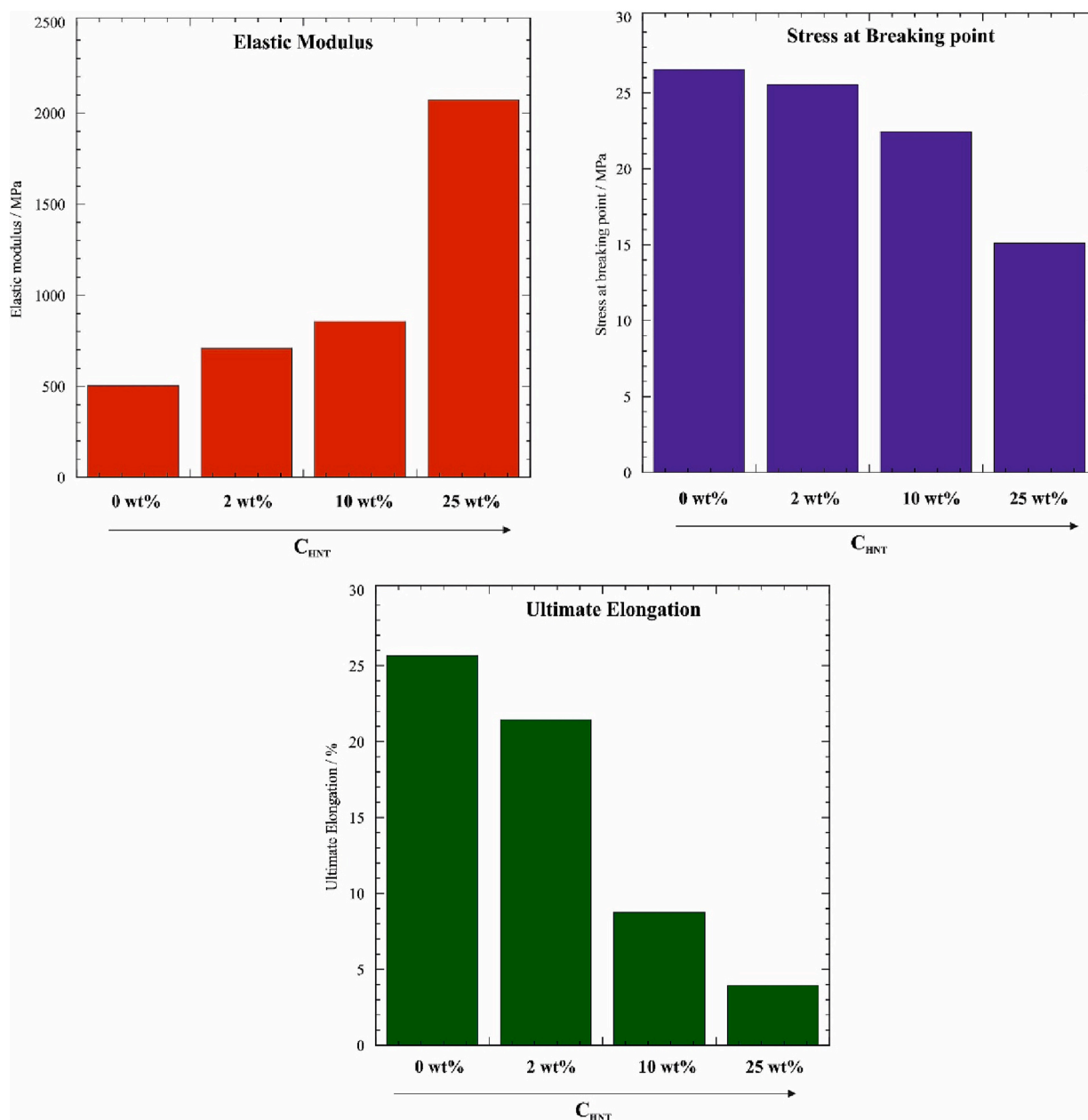
Fig. 6. Tensile properties of Funori/HNT nanocomposite films with variable filler content.

Table 2
Viscoelastic parameters of the Funori based films obtained by DMA oscillatory experiments.

Film	G' (25 °C)/ MPa	G" (25 °C)/ MPa	Tan(δ) (25 °C)	Temperature at tan (δ) peak/°C
Funori	1676	233	0.139	74.6
Funori/HNT (C_{HNT} = 2 wt %)	1695	235	0.138	66.7
Funori/HNT (C_{HNT} = 10 wt %)	1829	250	0.136	62.8
Funori/HNT (C_{HNT} = 25 wt %)	2038	270	0.132	59.6

Then, we employed the loaded nanotubes as fillers for Funori matrix allowing us to obtain films with antimicrobial/anti-inflammatory properties, which can be controlled over time. In this regard, the release kinetics of sodium diclofenac from composite films with variable composition (C_{HNT} = 10 and 25 wt%) were investigated in aqueous medium at pH = 6. Moreover, we studied the drug release from the loaded halloysite nanotubes under the same conditions. The drug release trends are presented in Fig. 9.

The release from the nanocomposite films evidenced an induction time (ca. 3 h), which was not observed for the drug delivery from halloysite nanotubes. This effect is related to the Funori solubilization in water that postpones the initial time of the sodium diclofenac release. It is important to evidence that the capacity to sustain the drug release can be exploited to develop oral dissolving films suitable in pharmaceutics [53]. As shown in Fig. 9, the complete release of sodium diclofenac is reached after ca. 30 h for both nanocomposites. The kinetic release (R%) data from 0 to 80 % were successfully fitted using the Korsmeyer-Peppas equation (Fig. 8), which can be expressed as.
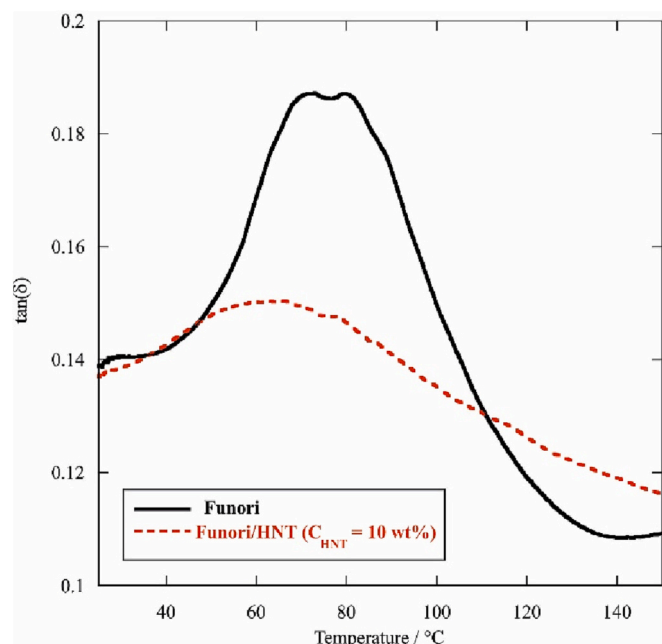
Fig. 7. Dependence of tan(δ) on temperature for films based on pristine Funori and Funori/HNT with halloysite content of 10 wt%.

$$R\% = k_{K-P} \cdot t^n \qquad (3)$$

being k_{K-P} the kinetic constant, while n is the exponential parameter related to the mechanism of the release process. Regarding the release from Funori/HNT films, the initial time ($t = 0$) is taken after the induction period related to the Funori solubilization. Table 3 collects the fitting parameters obtained from the analysis of the release trends by Korsmeyer-Peppas model. We observed that the drug release from HNT can be ascribed to a non-Fickian diffusion mechanism being that n is larger than 0.43 [54]. Similar observations are reported for the ibuprofen release in water from APTES modified halloysite [55] as well as for the doxycycline release in aqueous medium from alginate nanohydrogels confined within the HNT cavity [56]. The release mechanism from the composite films can be attributed to a Fickinan diffusion being that the estimated n values are lower than 0.43. Similar results were observed for the release of salycilic acid from pectin/HNT nanocomposites [36]. Based on both fitting parameters, we calculated that the kinetic constant is 1.34 min^{-1} for halloysite, while k_{K-P} are 2.57 and 2.51 min^{-1} for Funori HNT nanocomposites with $C_{HNT} = 10$ and 25 wt %, respectively. These results highlight the release is slower from the films compared to pure halloysite and the filler content does not significantly affect the release kinetics for the Funori/HNT nanocomposites.

4. Conclusions

Nanocomposite films based on Funori and halloysite clay nanotubes were successfully prepared by means of the aqueous casting procedure. We detected that the halloysite content in the composite materials
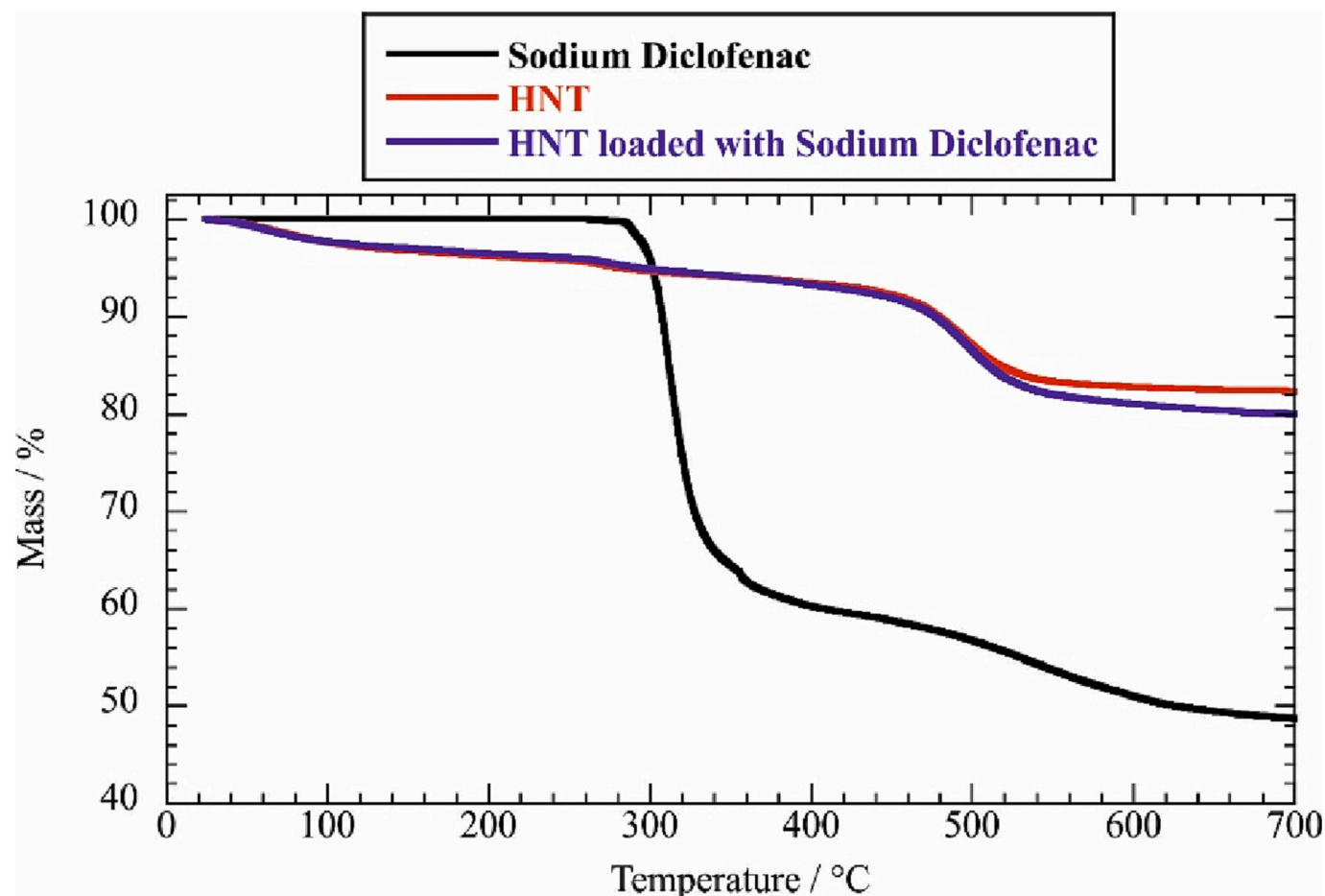

Fig. 8. Thermogravimetric curves of HNT, sodium diclofenac and HNT loaded with sodium diclofenac.
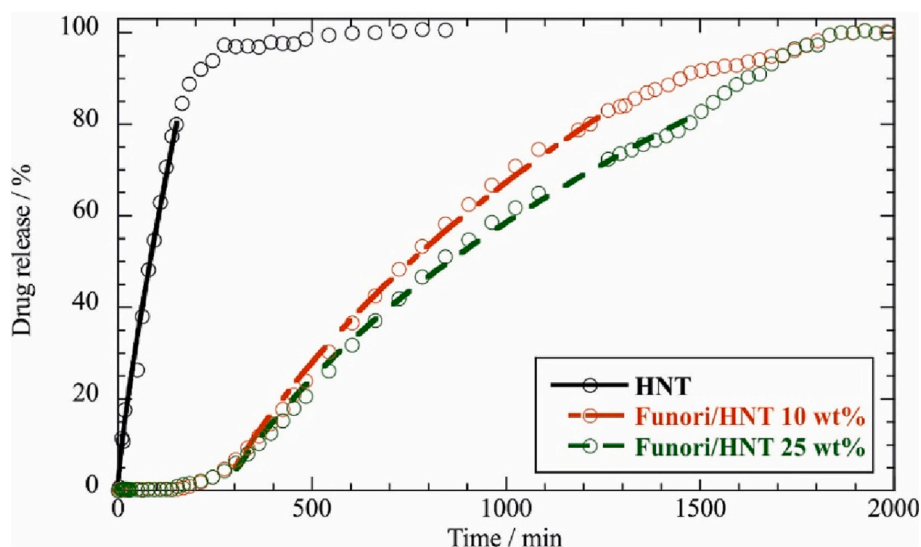
Fig. 9. Kinetics of sodium diclofenac release from HNT and Funori/HNT composite films with variable halloysite content. The lines represent the fitting curves of the release data between 0 and 80 % according to Korsmeyer-Peppas equation.

Table 3
Kinetic parameters for sodium diclofenac release obtained by Korsmeyer-Peppas model.

Delivery system	n	k_{K-P} / min^{-n}
HNT	0.79 ± 0.07	1.46 ± 0.18
Funori/HNT ($C_{HNT} = 10$ wt%)	0.37 ± 0.06	12.9 ± 1.9
Funori/HNT ($C_{HNT} = 25$ wt%)	0.34 ± 0.06	15 ± 2

significantly affects the wettability and optical properties of the films because of the different morphological characteristics, which were evidenced by SEM images. In general, the light attenuation coefficient was enhanced by increasing the nanofiller concentration. The Funori filling with small amounts of halloysite generated a decrease of the initial water contact angle highlighting a surface hydrophilization of the polymeric film due to the presence of homogeneously dispersed halloysite nanotubes at the interface. This effect was observed for halloysite concentration up to 15 wt%, while a further addition of the nanofiller did not induce any variations on the wettability because of the formation of clusters between the nanotubes. The presence of halloysite nanotubes within the Funori matrix altered the tensile properties of the films in terms of elastic modulus, stress at break and ultimate elongation. The Funori filling with halloysite improved the elastic modulus with an enhancement up to 300 % for the largest investigated filler content (25 wt%). On the other hand, stress and elongation at breaking point exhibited a decreasing trend with the halloysite concentration. According to the tensile experiments in the oscillatory regime, we observed that the presence of clay nanotubes decreased the glass transition temperature and the heat storage capacity of Funori.

Furthermore, we explored the suitability of the Funori based films for pharmaceutical applications by filling the polymeric matrix with modified halloysite nanotubes containing sodium diclofenac. To this purpose, the halloysite cavity was loaded with the drug by using the vacuum assisted procedure. In vitro release experiments in aqueous medium evidenced that the drug delivery from Funori/halloysite nanocomposites starts after an induction time of ca. 3 h, which is related to the polymer solubilization in water. This effect is promising to develop oral dissolving films with sustained drug release capacity. The release data between 0 and 80 % were successfully analyzed by the Korsmeyer-Peppas equation, which revealed that the drug delivery from the Funori/halloysite composite films is consistent with the Fickinan diffusion mechanism. In addition, we observed that the kinetic constant

of the release process from the nanocomposite films is slightly affected by the halloysite concentration.

In conclusion, this paper demonstrates that the combination of Funori and halloysite nanotubes can be perspective to develop functional nanocomposite films with variable physico-chemical properties on dependence of the filler content.

CRediT authorship contribution statement

Giuseppe Cavallaro: Investigation, Data curation, Writing- Original draft preparation. Writing- Reviewing and Editing, Validation. **Giuseppe Lazzara:** Conceptualization, Supervision.**Stefana Milioto:** Funding acquisition, Resources.

Declaration of competing interest

The authors declare that they have no known competing financial interests or personal relationships that could have appeared to influence the work reported in this paper.

Acknowledgments

References

[1] M. Liu, R. Fakhrullin, A. Novikov, A. Panchal, Y. Lvov, Tubule nanoclay-organic heterostructures for biomedical applications, Macromol. Biosci. 19 (2019), 1800419, https://doi.org/10.1002/mabi.201800419.

[2] E.P. Rebitski, M. Darder, R. Carraro, P. Aranda, E. Ruiz-Hitzky, Chitosan and pectin core–shell beads encapsulating metformin–clay intercalation compounds for controlled delivery, New J. Chem. 44 (2020) 10102–10110, https://doi.org/10.1039/C9NJ06433H.

[3] G.P. Udayakumar, S. Muthusamy, B. Selvaganesh, N. Sivarajasekar, K. Rambabu, F. Banat, S. Sivamani, N. Sivakumar, A. Hosseini-Bandegharaei, P.L. Show, Biopolymers and composites: properties, characterization and their applications in food, medical and pharmaceutical industries, J. Environ. Chem. Eng. 9 (2021), 105322, https://doi.org/10.1016/j.jece.2021.105322.

[4] X. Yang, Y. Zhang, D. Zheng, J. Yue, M. Liu, Nano-biocomposite films fabricated from cellulose fibers and halloysite nanotubes, Appl. Clay Sci. 190 (2020), 105565, https://doi.org/10.1016/j.clay.2020.105565.

[5] Y. Wang, S. Yi, R. Lu, D.E. Sameen, S. Ahmed, J. Dai, W. Qin, S. Li, Y. Liu, Preparation, characterization, and 3D printing verification of chitosan/halloysite nanotubes/tea polyphenol nanocomposite films, Int. J. Biol. Macromol. 166 (2021) 32–44, https://doi.org/10.1016/j.ijbiomac.2020.09.253.

[6] G. Cavallaro, M.R. Caruso, S. Milioto, R. Fakhrullin, G. Lazzara, Keratin/alginate hybrid hydrogels filled with halloysite clay nanotubes for protective treatment of human hair, Int. J. Biol. Macromol. 222 (2022) 228–238, https://doi.org/10.1016/j.ijbiomac.2022.09.170.

[7] Y. Lvov, A. Aerov, R. Fakhrullin, Clay nanotube encapsulation for functional biocomposites, Adv. Colloid Interf. Sci. 207 (2014) 189–198, https://doi.org/10.1016/j.cis.2013.10.006.

[8] A.C. Santos, I. Pereira, S. Reis, F. Veiga, M. Saleh, Y. Lvov, Biomedical potential of clay nanotube formulations and their toxicity assessment, Expert Opin. Drug Deliv. 16 (2019) 1169–1182, https://doi.org/10.1080/17425247.2019.1665020.

[9] A.C. Santos, C. Ferreira, F. Veiga, A.J. Ribeiro, A. Panchal, Y. Lvov, A. Agarwal, Halloysite clay nanotubes for life sciences applications: from drug encapsulation to bioscaffold, Adv. Colloid Interf. Sci. 257 (2018) 58–70, https://doi.org/10.1016/j.cis.2018.05.007.

[10] Y. Feng, X. Zhou, J. Yang, X. Gao, L. Yin, Y. Zhao, B. Zhang, Encapsulation of ammonia borane in Pd/Halloysite nanotubes for efficient thermal dehydrogenation, ACS Sustain. Chem. Eng. 8 (2020) 2122–2129, https://doi.org/10.1021/acssuschemeng.9b04480.

[11] Y. Liu, H. Guan, J. Zhang, Y. Zhao, J.-H. Yang, B. Zhang, Polydopamine-coated halloysite nanotubes supported AgPd nanoalloy: an efficient catalyst for hydrolysis of ammonia borane, Int. J. Hydrog. Energy 43 (2018) 2754–2762, https://doi.org/10.1016/j.ijhydene.2017.12.105.

[12] S. Sadjadi, M.M. Heravi, S.S. Kazemi, Ionic liquid decorated chitosan hybridized with clay: a novel support for immobilizing pd nanoparticles, Carbohydr. Polym. 200 (2018) 183–190, https://doi.org/10.1016/j.carbpol.2018.07.093.

[13] S. Sadjadi, M. Malmir, M.M. Heravi, F.G. Kahangi, Biocompatible starch-halloysite hybrid: an efficient support for immobilizing pd species and developing a heterogeneous catalyst for ligand and copper free coupling reactions, Int. J. Biol. Macromol. 118 (2018) 1903–1911, https://doi.org/10.1016/j.ijbiomac.2018.07.053.

[14] O. Owoseni, Y. Su, S. Raghavan, A. Bose, V.T. John, Hydrophobically modified chitosan biopolymer connects halloysite nanotubes at the oil-water interface as complementary pair for stabilizing oil droplets, J. Colloid Interface Sci. 620 (2022) 135–143, https://doi.org/10.1016/j.jcis.2022.03.142.

[15] O. Owoseni, E. Nyankson, Y. Zhang, S.J. Adams, J. He, G.L. McPherson, A. Bose, R. B. Gupta, V.T. John, Release of surfactant cargo from interfacially-active halloysite clay nanotubes for oil spill remediation, Langmuir 30 (2014) 13533–13541, https://doi.org/10.1021/la503687b.

[16] R. von Klitzing, D. Stehl, T. Pogrzeba, R. Schomäcker, R. Minullina, A. Panchal, S. Konnova, R. Fakhrullin, J. Koetz, H. Möhwald, Y. Lvov, Halloysites stabilized emulsions for hydroformylation of long chain olefins, Adv. Mater. Interfaces (2016), https://doi.org/10.1002/admi.201600435, 1600435-n/a.

[17] A. Panchal, L.T. Swientoniewski, M. Omarova, T. Yu, D. Zhang, D.A. Blake, V. John, Y.M. Lvov, Bacterial proliferation on clay nanotube Pickering emulsions for oil spill bioremediation, Colloids Surf. B Biointerfaces. 164 (2018) 27–33, https://doi.org/10.1016/j.colsurfb.2018.01.021.

[18] F. Persano, S. Batasheva, G. Fakhrullina, G. Gigli, S. Leporatti, R. Fakhrullin, Recent advances in the design of inorganic and nano-clay particles for the treatment of brain disorders, J. Mater. Chem. B 9 (2021) 2756–2784, https://doi.org/10.1039/D0TB02957B.

[19] A. Vikulina, D. Voronin, R. Fakhrullin, V. Vinokurov, D. Volodkin, Naturally derived nano- and micro-drug delivery vehicles: halloysite, vaterite and nanocellulose, New J. Chem. 44 (2020) 5638–5655, https://doi.org/10.1039/C9NJ06470B.

[20] X. Zhao, C. Zhou, M. Liu, Self-assembled structures of halloysite nanotubes: towards the development of high-performance biomedical materials, J. Mater. Chem. B 8 (2020) 838–851, https://doi.org/10.1039/C9TB02460C.

[21] A.M. Yamina, M. Fizir, A. Itatahine, H. He, P. Dramou, Preparation of multifunctional PEG-graft-halloysite nanotubes for controlled drug release, tumor cell targeting, and bio-imaging, Colloids Surf. B Biointerfaces 170 (2018) 322–329, https://doi.org/10.1016/j.colsurfb.2018.06.042.

[22] Q. Li, X. Hu, P. Perkins, T. Ren, Antimicrobial film based on poly(lactic acid) and natural halloysite nanotubes for controlled cinnamaldehyde release, Int. J. Biol. Macromol. 224 (2023) 848–857, https://doi.org/10.1016/j.ijbiomac.2022.10.171.

[23] E. Rozhina, S. Batasheva, R. Miftakhova, X. Yan, A. Vikulina, D. Volodkin, R. Fakhrullin, Comparative cytotoxicity of kaolinite, halloysite, multiwalled carbon nanotubes and graphene oxide, Appl. Clay Sci. 205 (2021) 106041, https://doi.org/10.1016/j.clay.2021.106041.

[24] X. Wang, J. Gong, Z. Gui, T. Hu, X. Xu, Halloysite nanotubes-induced Al accumulation and oxidative damage in liver of mice after 30-day repeated oral administration, Environ. Toxicol. 33 (2018) 623–630, https://doi.org/10.1002/tox.22543.

[25] E.A. Naumenko, I.D. Guryanov, R. Yendluri, Y.M. Lvov, R.F. Fakhrullin, Clay nanotube–biopolymer composite scaffolds for tissue engineering, Nanoscale 8 (2016) 7257–7271, https://doi.org/10.1039/C6NR00641H.

[26] Y. Zhang, R. Meng, J. Zhou, X. Liu, W. Guo, Halloysite nanotubes-decorated electrospun biobased polyamide scaffolds for tissue engineering applications, Colloids Surf. Physicochem. Eng. Asp. 648 (2022), 129378, https://doi.org/10.1016/j.colsurfa.2022.129378.

[27] M. Liu, C. Wu, Y. Jiao, S. Xiong, C. Zhou, Chitosan-halloysite nanotubes nanocomposite scaffolds for tissue engineering, J. Mater. Chem. B 1 (2013) 2078–2089, https://doi.org/10.1039/C3TB20084A.

[28] C. Cheng, Y. Gao, W. Song, Q. Zhao, H. Zhang, H. Zhang, Halloysite nanotube-based H2O2-responsive drug delivery system with a turn on effect on fluorescence for real-time monitoring, Chem. Eng. J. 380 (2020) 122474, https://doi.org/10.1016/j.cej.2019.122474.

[29] F. Liu, L. Bai, H. Zhang, H. Song, L. Hu, Y. Wu, X. Ba, Smart H2O2-responsive drug delivery system made by halloysite nanotubes and carbohydrate polymers, ACS Appl. Mater. Interfaces 9 (2017) 31626–31633, https://doi.org/10.1021/acsami.7b10867.

[30] L. Lisuzzo, G. Cavallaro, S. Milioto, G. Lazzara, Halloysite nanotubes filled with salicylic acid and sodium diclofenac: effects of vacuum pumping on loading and release properties, J. Nanostructure Chem. 11 (2021) 663–673, https://doi.org/10.1007/s40097-021-00391-z.

[31] M. Liu, Y. Chang, J. Yang, Y. You, R. He, T. Chen, C. Zhou, Functionalized halloysite nanotube by chitosan grafting for drug delivery of curcumin to achieve enhanced anticancer efficacy, J. Mater. Chem. B 4 (2016) 2253–2263, https://doi.org/10.1039/C5TB02725J.

[32] A. Spepi, C. Duce, A. Pedone, D. Presti, J.-G. Rivera, V. Ierardi, M.R. Tiné, Experimental and DFT characterization of halloysite nanotubes loaded with salicylic acid, J. Phys. Chem. C 120 (2016) 26759–26769, https://doi.org/10.1021/acs.jpcc.6b06964.

[33] M. Fizir, P. Dramou, N.S. Dahiru, W. Ruya, T. Huang, H. He, Halloysite nanotubes in analytical sciences and in drug delivery: a review, Microchim. Acta 185 (2018) 389, https://doi.org/10.1007/s00604-018-2908-1.

[34] L. Lisuzzo, G. Cavallaro, S. Milioto, G. Lazzara, Layered composite based on halloysite and natural polymers: a carrier for the pH controlled release of drugs, New J. Chem. 43 (2019) 10887–10893, https://doi.org/10.1039/C9NJ02565K.

[35] N. Khatoon, M.Q. Chu, C.H. Zhou, Nanoclay-based drug delivery systems and their therapeutic potentials, J. Mater. Chem. B 8 (2020) 7335–7351, https://doi.org/10.1039/D0TB01031F.

[36] M. Makaremi, P. Pasbakhsh, G. Cavallaro, G. Lazzara, Y.K. Aw, S.M. Lee, S. Milioto, Effect of morphology and size of halloysite nanotubes on functional pectin bionanocomposites for food packaging applications, ACS Appl. Mater. Interfaces 9 (2017) 17476–17488, https://doi.org/10.1021/acsami.7b04297.

[37] G. Biddeci, G. Cavallaro, F. Di Blasi, G. Lazzara, M. Massaro, S. Milioto, F. Parisi, S. Riela, G. Spinelli, Halloysite nanotubes loaded with peppermint essential oil as filler for functional biopolymer film, Carbohydr. Polym. 152 (2016) 548–557, https://doi.org/10.1016/j.carbpol.2016.07.041.

[38] E. Boccalon, P. Sassi, L. Pioppi, A. Ricci, M. Marinozzi, G. Gorrasi, M. Nocchetti, Onion skin extract immobilized on halloysite-layered double hydroxide filler as active pH indicator for food packaging, Appl. Clay Sci. 227 (2022), 106592, https://doi.org/10.1016/j.clay.2022.106592.

[39] G. Gorrasi, Dispersion of halloysite loaded with natural antimicrobials into pectins: characterization and controlled release analysis, Carbohydr. Polym. 127 (2015) 47–53, https://doi.org/10.1016/j.carbpol.2015.03.050.

[40] M. Barman, S. Mahmood, R. Augustine, A. Hasan, S. Thomas, K. Ghosal, Natural halloysite nanotubes /chitosan based bio-nanocomposite for delivering norfloxacin, an anti-microbial agent in sustained release manner, Int. J. Biol. Macromol. 162 (2020) 1849–1861, https://doi.org/10.1016/j.ijbiomac.2020.08.060.

[41] M. Akrami-Hasan-Kohal, M. Ghorbani, F. Mahmoodzadeh, B. Nikzad, Development of reinforced aldehyde-modified kappa-carrageenan/gelatin film by incorporation of halloysite nanotubes for biomedical applications, Int. J. Biol. Macromol. 160 (2020) 669–676, https://doi.org/10.1016/j.ijbiomac.2020.05.222.

[42] L. Lisuzzo, G. Cavallaro, S. Milioto, G. Lazzara, Effects of halloysite content on the thermo-mechanical performances of composite bioplastics, Appl. Clay Sci. 185 (2020), 105416, https://doi.org/10.1016/j.clay.2019.105416.

[43] N.T. Ha, C.H. Ha, N. Hayakawa, R. Chujo, S. Kawahara, Relationship between structure and some physico-chemical properties of funori from red seaweed gloiopeltis, J. Cult. Herit. 51 (2021) 14–20, https://doi.org/10.1016/j.culher.2021.06.010.

[44] G.F. Bettina, B. Giambra, G. Cavallaro, G. Lazzara, B. Megna, R. Fakhrullin, F. Akhatova, R. Fakhrullin, Restoration of a XVII Century's predella reliquary: from physico-chemical characterization to the conservation process, Forests 12 (2021), https://doi.org/10.3390/f12030345.

[45] V. Bertolino, G. Cavallaro, G. Lazzara, M. Merli, S. Milioto, F. Parisi, L. Sciascia, Effect of the biopolymer charge and the nanoclay morphology on nanocomposite materials, Ind. Eng. Chem. Res. 55 (2016) 7373–7380, https://doi.org/10.1021/acs.iecr.6b01816.

[46] D. Huang, M. Sun, Y. Bu, F. Luo, C. Lin, Z. Lin, Z. Weng, F. Yang, D. Wu, Microcapsule-embedded hydrogel patches for ultrasound responsive and enhanced transdermal delivery of diclofenac sodium, J. Mater. Chem. B 7 (2019) 2330–2337, https://doi.org/10.1039/C8TB02928H.

[47] A. Marmur, From hygrophilic to superhygrophobic: theoretical conditions for making high-contact-angle surfaces from low-contact-angle materials, Langmuir 24 (2008) 7573–7579, https://doi.org/10.1021/la800304r.

[48] S. Farris, L. Introzzi, P. Biagioni, T. Holz, A. Schiraldi, L. Piergiovanni, Wetting of biopolymer coatings: contact angle kinetics and image analysis investigation, Langmuir 27 (2011) 7563–7574, https://doi.org/10.1021/la2017006.

[49] V. Bertolino, G. Cavallaro, S. Milioto, G. Lazzara, Polysaccharides/Halloysite nanotubes for smart bionanocomposite materials, Carbohydr. Polym. 245 (2020), 116502, https://doi.org/10.1016/j.carbpol.2020.116502.

[50] G. Cavallaro, G. Lazzara, S. Milioto, Dispersions of nanoclays of different shapes into aqueous and solid biopolymeric matrices. extended physicochemical study, Langmuir 27 (2011) 1158–1167, https://doi.org/10.1021/la103487a.

[51] X. Tang, S. Alavi, Structure and physical properties of Starch/Poly vinyl Alcohol/Laponite RD nanocomposite films, J. Agric. Food Chem. 60 (2012) 1954–1962, https://doi.org/10.1021/jf2024962.

[52] M. Liu, Y. Zhang, C. Wu, S. Xiong, C. Zhou, Chitosan/halloysite nanotubes bionanocomposites: structure, mechanical properties and biocompatibility, Int. J.

Biol. Macromol. 51 (2012) 566–575, https://doi.org/10.1016/j.
ijbiomac.2012.06.022.

[53] M.A. Bonsu, K. Ofori-Kwakye, S.L. Kipo, M.E. Boakye-Gyasi, M.-A. Fosu, Development of Oral dissolvable films of diclofenac sodium for osteoarthritis using albizia and khaya gums as hydrophilic film formers, J. Drug Deliv. 2016 (2016), 6459280, https://doi.org/10.1155/2016/6459280.

[54] P.L. Ritger, N.A. Peppas, A simple equation for description of solute release I. Fickian and non-fickian release from non-swellable devices in the form of slabs,

spheres, cylinders or discs, J. Control. Release 5 (1987) 23–36, https://doi.org/10.1016/0168-3659(87)90034-4.

[55] D. Tan, P. Yuan, F. Annabi-Bergaya, D. Liu, L. Wang, H. Liu, H. He, Loading and in vitro release of ibuprofen in tubular halloysite, Appl. Clay Sci. 96 (2014) 50–55, https://doi.org/10.1016/j.clay.2014.01.018.

[56] G. Cavallaro, G. Lazzara, S. Milioto, F. Parisi, V. Evtugyn, E. Rozhina, R. Fakhrullin, Nanohydrogel formation within the halloysite lumen for triggered and sustained release, ACS Appl. Mater. Interfaces 10 (2018) 8265–8273, https://doi.org/10.1021/acsami.7b19361.